Supporting Information

Multivalency at Interfaces: Supramolecular Carbohydrate-Functionalized Graphene Derivatives for Bacterial Capture, Release and Disinfection

Zhenhui Qi,[†,#] *Priya Bharate,*[‖,‡, #] *Chian-Hui Lai,*[‖,‡] *Benjamin Ziem,*[†] *Christoph Böttcher,*[§] *Andrea Schulz,*[§] *Fabian Beckert,*[⊥] *Benjamin Hatting,*[▵] *Rolf Mülhaupt,*[⊥] *Peter H. Seeberger,*[*,‖,‡] *and Rainer Haag*[*, †]

[†]Institut für Chemie und Biochemie, Freie Universität Berlin, Takustrasse 3, 14195, Berlin, Germany

[‖]Biomolecular Systems Department, Max Planck Institute of Colloids and Interfaces, Am Mühlenberg 1, 14476 Potsdam, Germany

[‡]Institute of Chemistry and Biochemistry, Freie Universität Berlin, Arnimallee 22, 14195 Berlin, Germany

[§]Research Center for Electron Microscopy and Core Facility BioSupraMol, Institut für Chemieund Biochemie, Freie Universität Berlin, Fabeckstr. 36a, 14195, Berlin, Germany

[⊥]Freiburg Materials Research Center (FMF) and Institute for Macromolecular Chemistry of the University of Freiburg, Stefan-Meier-Strasse 31, D-79104 Freiburg, Germany

[▵] Fachbereich Physik, Freie Universität Berlin, Arnimallee 14, 14195 Berlin, Germany

Table of content

1. General methods

All reagents were commercially available and used as supplied without further purification. Solvents were either employed as purchased or dried prior to use by usual laboratory methods. NMR data were obtained on Bruker ECX 400 MHz, Jeol Eclipse 500 MHz, or Bruker AVANCE III 700 MHz NMR spectrometers, FTIR spectra recorded on a Nicolet Avatar 320 FT-IR spectrometer. UV/Vis spectra recorded on a Varian Cary 50 Bio UV/Vis spectrophotometer. Thermogravimetric analysis (TGA) of samples were performed on TGA/SDTA 851 (Mettler/Toledo, Gießen, Germany) at temperatures varied from 30 ℃ to 700 ℃ using a heating rate of 10 K min^{-1} (with purge gas flow of 20 mL min^{-1} nitrogen). Mass spectra were obtained using an electrospray ionization (ESI) interface on an Agilent LC/MSD TOF system. The AFM measurements have been performed using a Nanoscope Multimode V (Veeco, now Bruker AXS, Mannheim). All images were flattened previous to height analysis using algorithms contained in the software NanoScope version 1.5. Tip convolution makes lateral dimension analysis difficult. Measurements were performed in laboratory air at room temperature. The microscope was operated in the tapping mode (TM-AFM) using silicone probes, PPP-NCL-R (NanoAndMor GmbH, Wetzlar), SNL-D and SNL-A (Bruker AXS GmbH, Karlsruhe) under ambient conditions. The cantilever was forced to oscillate near its resonance frequency. The samples were prepared by spin coating (Spin Coater SCV-2) at 5000 rpm for 300s on freshly cleaved mica.

Preparation of supramolecular inclusion complexes ManCD@AG4 and CD@AG4. Typically, 0.5 mg AG4 ($n_{adamantyl\ unit}$ = 0.217 μmol) was dissolved in 200 μL DMF with the assistance of ultrasonication (10 min). After that, 1 mg ManCD ($n_{ß\text{-}cyclodextrin}$ unit = 0.371 μmol) dissolved in 200 μL Milli-Q water was injected into the solution of AG4. The mixtures were sonicated for 30 min to aid the complexation process. The sample vial was left for 16 h at ambient condition before the addition of 500 μL water. The DMF and excess ManCD were removed by centrifugation for twice (12000 rpm, 10 min). The final centrifugal precipitation was collected and re-suspended in 600 μL water, affording the supramolecular carbohydrate functionalized graphene ManCD@AG4. The preparation of CD@AG4 was carried out under the identical protocol, except using 0.421 mg ß-cyclodextrin (ßCD, 0.371 μmol).

E.coli microscopy experiment and proliferation assay. *E.coli* strain bearing a mannose-binding protein (ORN178) and a mutant strain lacking the mannose binding domain (ORN208) were grown at 37 ℃ in Luria-Bertani (LB) medium (5 mL) to an OD_{600} of ~1.0 (1×10^8 CFU/mL). For different assays both strains were washed and appropriate dilutions made in phosphate-buffered saline (PBS, pH 7.4).

Confocal laser scanning microscope (CLSM) images. A solution of either ManCD@AG4 or CD@AG4 (10 μL, 16.33 μM) was coated on poly-l-lysine slide. In order to avoid dust contamination, the slide was kept in slide cover box at room temperature and further stored at 4 ℃ overnight. The fluorescent dye-labeled *E.coli* strains were prepared as following: 100 μL of a FITC (Fluorescein isothiocyanate) solution (1 mg/mL) was added to the 2 mL solution of *E.coli* strain ORN178 or ORN208 (10^7 CFU mL^{-1}) in PBS. The mixture was incubated at 4 ℃ for 1 h and washed three times with PBS. 10 μL FITC-labeled *E.coli* were added on coated slide and incubated at 37 ℃ for 1 h. The cells were washed three times with PBS and then visualized on a confocal microscope LSM700 (Zeiss, Leipzig, Germany).

Transmission electron microscopy (TEM) images. Droplets (~5 μL) of ManCD@AG4 sample solution were placed on carbon film coated copper grids (Plano GmbH, Wetzlar, Germany) and supernatant liquid was removed by blotting with a piece of filter paper. The grids were allowed to air-dry at least 40 min and were subsequently transferred into the microscope without use of a contrasting or cryo-fixation step (Note: graphene and its derivatives are known to create sufficient contrast in the TEM on their own).

Release the captured E.coli by competitive guests. 27 μL stock solution of ManCD@AG4 (98.2 μM) was diluted 420 μL by PBS buffer, and divided into two portions (210 μL for each). Each portion was added 45 μL FITC stained *E.coli* stain ORN178 solution. The mixture was incubated at room temperature for 1 h on the orbital shaker with gentle shaking. 40 μL solution of incubated sample was taken out and revered for recording starting fluorescent intensity (FI). After that, one portion of *E.coli* captured sample was injected by 28 μL solution of concentrated competitive

guest, such as sodium adamantine carboxylate (AdCNa) or methyl α-D-mannopyranoside (Me-Man). The other portion was injected by 20 μL PBS as control. Both portions were further gentlely shaked on the obitalsher for another 1 h. Afterwards, both sampes were left still for 10 min, and 40 μL supernatant was taken out from the upper layer of sample, and checked the FI by fluorescence reader. The amount of released *E.coli* was calculated according to the variation of FI.

Near Infrared (NIR) treatment for bacteria disinfection. The solution of *E.coli* strain ORN178 45 μL (OD_{600} = 0.3, ~10^6 CFU/mL, in PBS) was mixed with 255 μL of stock solution of ManCD@AG4 or CD@AG4 (ManCD in 98.2 μM, AG4 in 0.83 mg/mL). The mixture was incubated respectively at room temperature for 1 h on the orbital shaker with gentle shaking. Afterwards, each mixture was immediately subjected to NIR laser irradiation (785 nm, 0.5 W/cm^2) for 10 min at a distance of 1 cm. Finally, 100 μL of irradiated sample was spread on agar plate, and incubated for 24 h at 37 ℃. In the diluted mode, the spreader which employed for spreading 100 μL irradiated sample was used directly without washing and spread again on agar plate. The control set was prepared by diluting 45 μL of bacteria to 255 μL with Milli-Q water and spread on agar plates.

2. Synthetic work

*2.1. Synthesis of compounds **1***

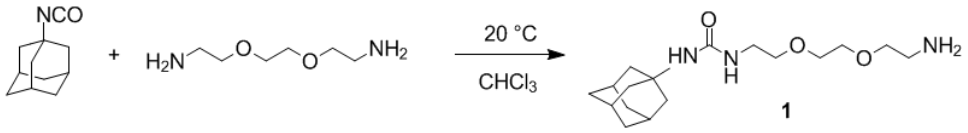

Scheme S1. Synthetic route to **1**.

Synthesis of **1**: 1-Adamantyl isocyanate (886 mg, 5 mmol) was dissolved in chloroform (10 mL) and added dropwise to a solution of 2,2'-(ethylenedioxy)bis(ethylamine) (14.82 g, 100 mmol) in chloroform (15 mL) at 0 °C. The suspension was stirred overnight at 20 °C. The reaction mixture was washed three times with water (100 mL), and the product was extracted by hydrochloric acid solution (100 mL 1 M in water). The aqueous layer was isolated, basified by addition of sodium hydroxide solution (10 mL 10 M in water), and subsequently extracted 3 times with dichloromethane (3 times 100 mL). The combined organic layers were dried with sodium sulfate and filtered, and the dichloromethane was removed under reduced pressure. Recrystallization of the product from diisopropyl ether gave the pure product as colorless crystals (yield: 80%). ^{1}H NMR (500 MHz, chloroform-*d*, room temperature) δ (ppm): 5.36 (t, J = 5.1 Hz, 1H), 5.24 (s, 1H), 3.60 – 3.54 (m, 2H), 3.53 – 3.46 (m, 2H), 3.27 (dd, J = 10.1, 5.1 Hz, 1H), 2.86 (t, J = 5.0 Hz, 1H), 2.44 (s, 1H), 1.99 (s, 1H), 1.90 (d, J = 2.8 Hz, 3H), 1.60 (s, 3H). The ^{13}C NMR spectrum of **1** is shown in Figure S2. ^{13}C NMR (126 MHz, chloroform-*d*, room temperature) δ (ppm): 157.89, 77.41, 77.16, 76.91, 72.33, 70.88, 70.05, 69.95, 50.59, 42.52, 41.43, 39.73, 36.53, 29.60. ESI-TOF-HRMS *m*/*z* calcd. for $[M+H]^+$ $C_{17}H_{32}N_3O_3$, 326.2438, found 326.2438.

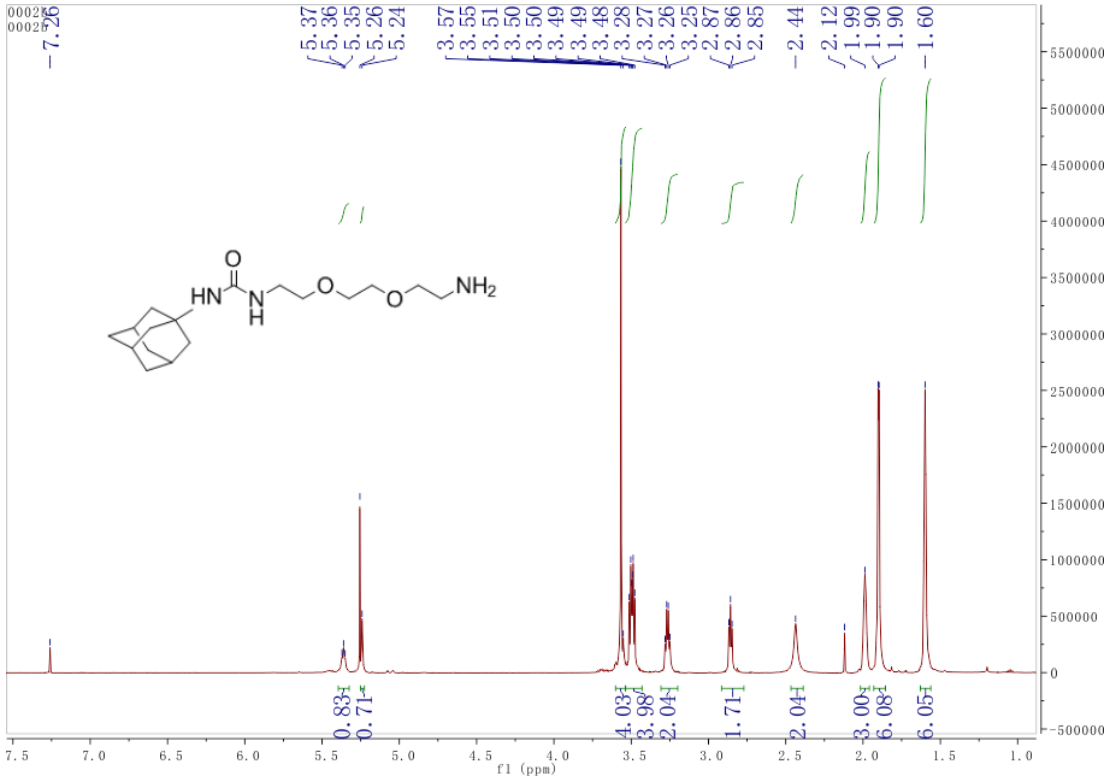

Figure S1. ^{1}H NMR spectrum (500 MHz, chloroform-*d*, room temperature) of **1**.

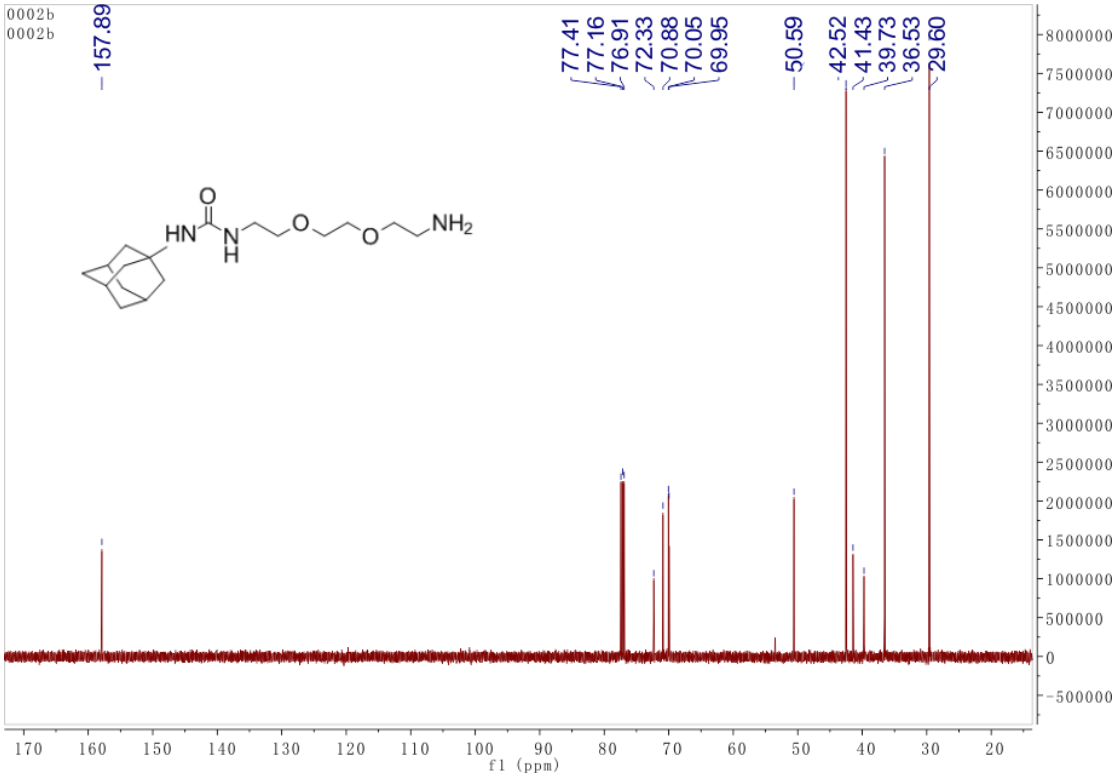

Figure S2. ^{13}C NMR spectrum (126 MHz, chloroform-*d*, room temperature) of **1**.

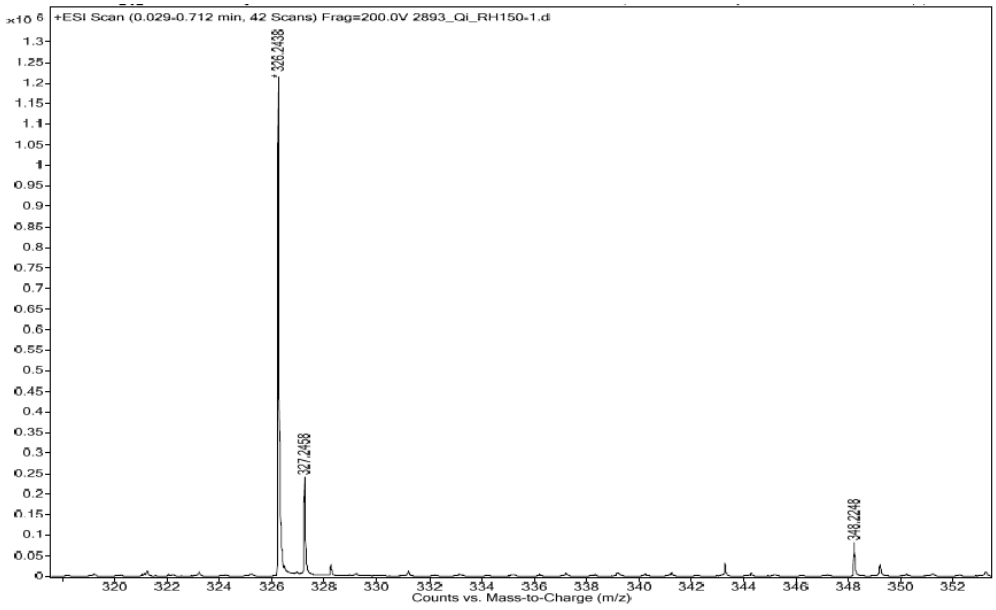

Figure S3. ESI-TOF mass spectrum of **1**.

*2.2. Synthesis of compound **2***

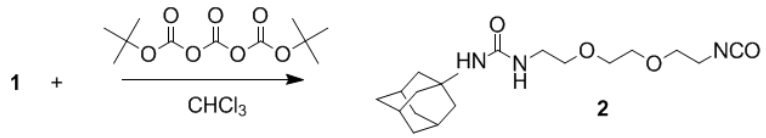

Scheme S2. Synthetic route to **2**.

Di-*tert*-butyl tricarbonate[1] (103 mg, 394 µmol) was dissolved in chloroform (4 mL), and **1** (128.2 mg, 394 µmol) in chloroform (4 mL) was injected in this solution at 20 °C. The reaction mixture was stirred for 30 min to yield isocyanate **2** which can be identified from the ^{1}H NMR shift. The isocyanate **2** was used directly for the next reaction without any purification. ^{1}H NMR (500 MHz, chloroform-*d*, room temperature) δ (ppm): 3.70 – 3.61 (m, 6H), 3.55 – 3.51 (m, 2H), 3.44 – 3.40 (m, 2H), 3.35 (s, 2H), 2.05 (s, 3H), 1.95 (d, J = 3.0 Hz, 3H), 1.65 (s, 3H).

2,3 Preparation of GO, TRGO400/750, AG4 and AG7

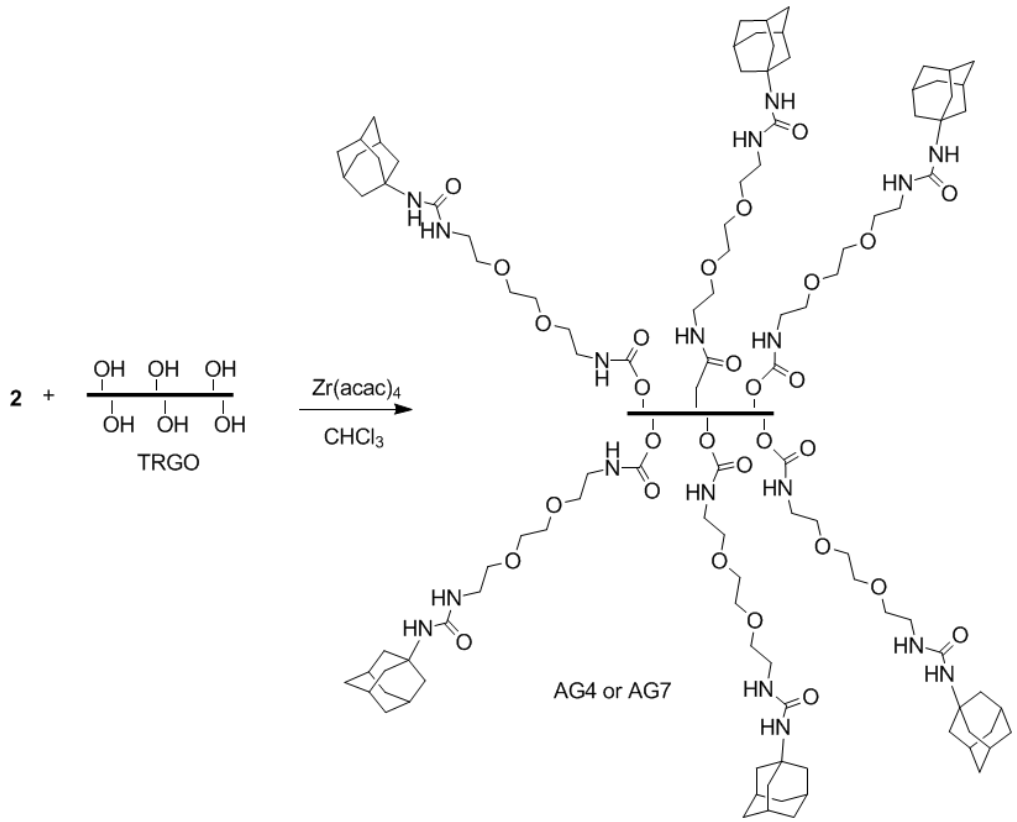

Scheme S3. Synthetic route to AG4 and AG7.

TRGO was produced in a two-step procedure starting with graphite. At first, the graphene oxide (GO) was prepared by oxidation of graphite according to the method of Hummers and Offemann.[2] Graphite (60 g) was stirred in concentrated H_2SO_4 (1.4 L) at room temperature and $NaNO_3$ (30 g) was added. The mixture was cooled to 0 ℃ and $KMnO_4$ (180 g) was added during 5 h. The reaction mixture was allowed to reach room temperature and stirred for 2 h. The reaction was quenched by pouring the reaction mixture into ice water (2 L) and adding H_2O_2 (3%, 200 mL). The GO was filtered off, washed with aqueous HCl (3%) and then with water until no AgCl precipitated when aqueous $AgNO_3$ was added to water. The purified chlorine-, sulfate- and manganese-free GO was dried in vacuum at 40 ℃ and powdered (60 mm mesh) by a ball mill (Retsch, Haan, Germany) using liquid nitrogen. In the second step, GO was thermally reduced at 400 ℃ or 750℃, to produce TRGO400 and TRGO750 respectively. TRGO 400/750 was obtained as a black powder of very low bulk density.

For the preparation of AG4, 40 mg TRGO400 (n_{-OH} = 64 μmol) was suspeneded in 5 mL dry

chloroform, and was consequently treated with an excess isocyanate solution **2** (15 mL) and 1 mg zirconium(IV) acetylacetonate ($Zr(acac)_2$) as catalyst in chloroform (50 mL). The mixture was stirred under argon for 3 day at a temperature of 40 ℃. AG4 was filtered off and washed several times with chloroform followed by drying in vacuum at 100 ℃.

2.4 Synthesis of ManCD

The synthesis of the mannose substituted β-cyclodextrin (ManCD) was started with known peracetylatedmannose **3** shown in scheme 4, glycosylated with bromoethanol in the presence of BF_3•OEt_2 yield **4**. Then **4** were converted to thiocyanate–mannose derivative **5** using KSCN. The thiocyanate **5** was reduced by Zn–AcOH to the corresponding thiol **6**. Iodinated cyclodextrin substrate **7** yields **8** after peracetylation. Then 6-hepta iodinated β-cyclodextrin **8** reacted with **6** in the presence of Cs_2CO_3 to yield mannose-substituted β-cyclodextrin **9**, which was finally treated with base yielding compound ManCD, as previously reported.[3]

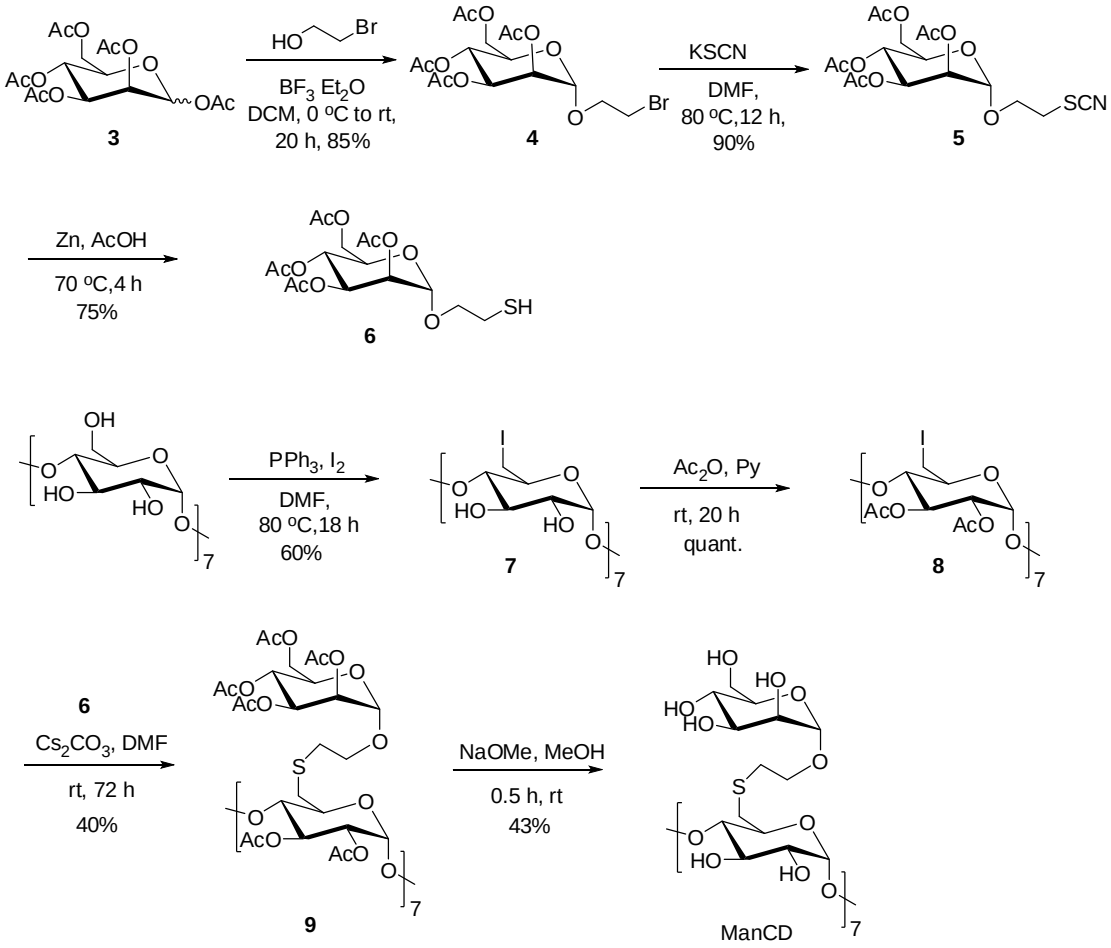

Scheme S4. Synthetic route to ManCD.

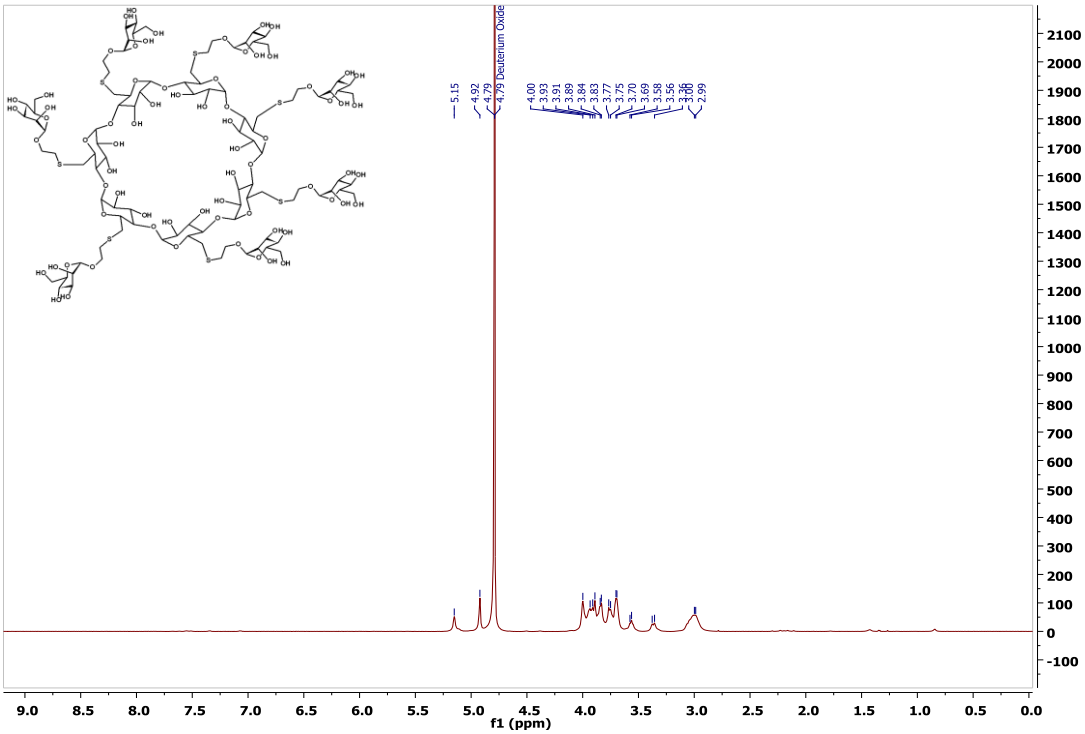

Figure S4. ^{1}H NMR spectrum (500 MHz, D_2O, room temperature) of ManCD.

3. Characterization of adamantyl-functionalized graphene derivatives

3.1 Elemental analysis

Table S1 Characterization of TRGO400/700 and AG4/AG7

Material	Elemental analysis		
	C [%]	H [%]	N [%]
TRGO750	85.78	0.58	—
AG7	81.79	1.25	0.65
TRGO400	80.9	1.2	—
AG4	65.98	3.27	1.26

The successful formation of the carbamate esters via the reaction of the isocyanate with the surface hydroxyls can be evidenced by the increased content of nitrogen (see Table S1). The TRGO400 provides higher densities of hydroxyl group on the carbon surface that can be functionalized: that is the -OH number in TRGO400 is 1.2 mol/kg; while the number in TRGO750

is 0.44 mol/kg. According to the carbon-to-nitrogen atomic ratio, one can estimate the approximate functionalization degree of adamantyl group attached. It is calculated that there is approximately 55 graphene carbons per one incorporated carbamate ester unit in AG4, which means 27 aromatic rings surrounding one adamantyl group.

3.2 IR spectra of GO, TRGO400, AG4

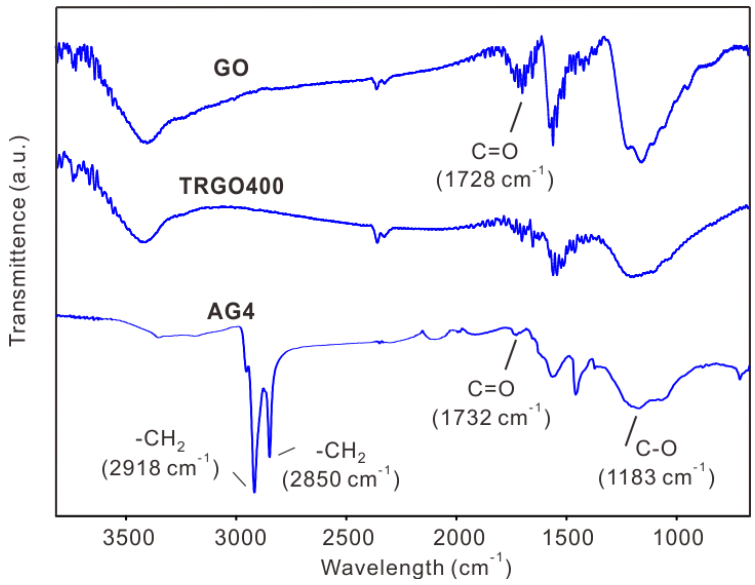

Figure S5. FT-IR spectra of GO, TRGO400 and adamantyl functionalized AG4. In the spectrum of AG4, the characteristic peak at 1732 cm^{-1} also increased, which is attributed to the C=O stretching of urethanes and provided evidence for successful chemical functionalization. At the same time, the intensity of the peaks associated to the $-CH_2$ stretching vibration at 2918 and 2850 cm^{-1} increased, as expected for the ethylenedioxy groups on TRGO surface.

3.3 Solubility test

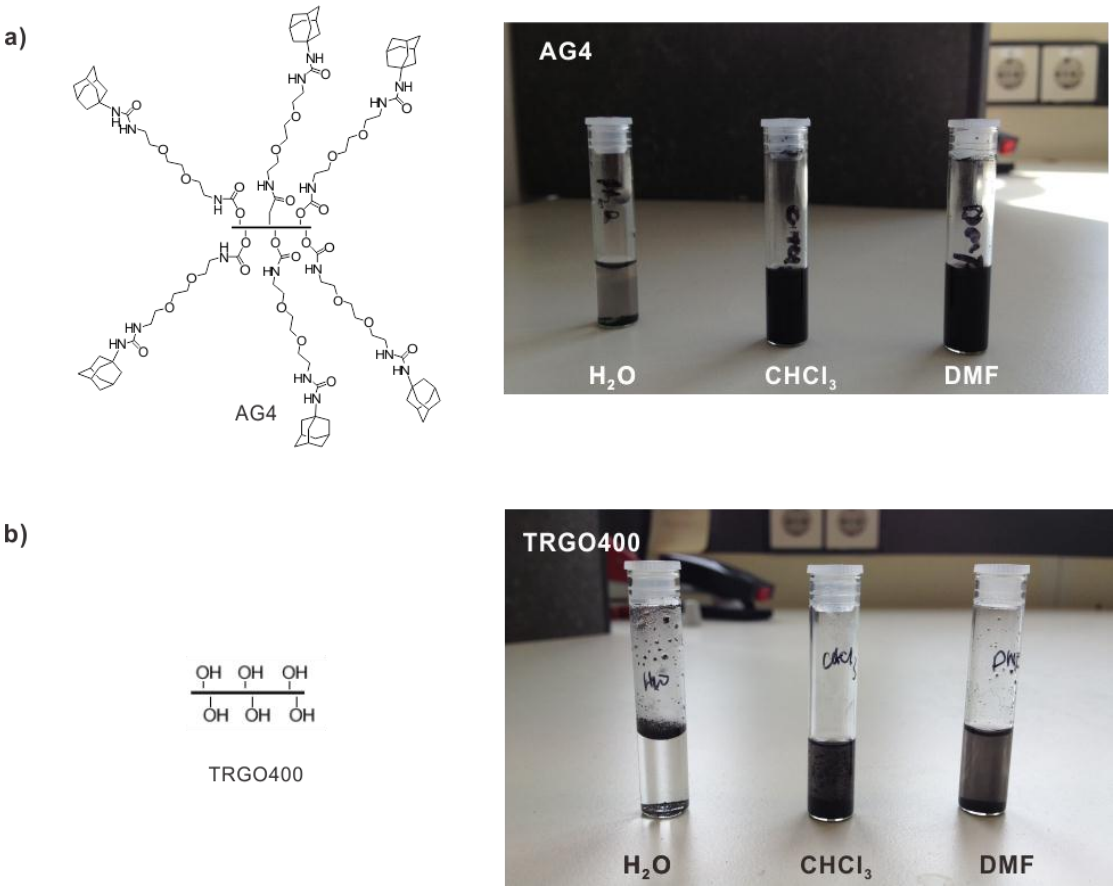

Figure S6. a) AG4 and b) TRGO400 dispersions in Milli-Q water, chloroform and DMF (1 mg/mL) 24 h after ultrasonication for 10 min. The image shows vials containing dispersions 24 h after preparation. In contrast to the parent TRGO400 (Figure S6b), adamantyl-functionalized AG4 readily forms stable colloidal dispersions chloroform and DMF. The improved solubility in organic mediums can be ascribed to the surface functionalization, which was also observed in other cases.[4]

3.4 TGA measurement

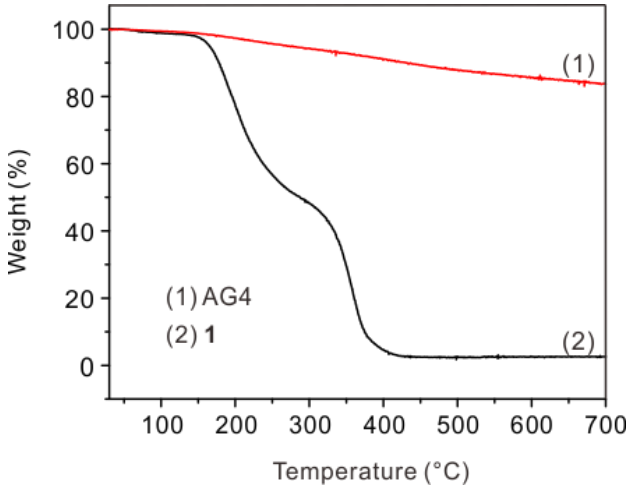

Figure S7. Thermogravimetric analysis (TGA) curves of the (1) AG4 and (3) **1**. It is found that compound **1** undergoes most of weight loss below 410 ℃. Our previous test shows the TGA curve of TRGO400 has 2% weight loss at temperature of 410 ℃.[5] This value for AG4 is 10.2%. Therefore, the amounts of decorated admantyl chain on the TRGO400 are calculated to be about 8.2%, which is in close to the value obtained from the elemental analysis that is 10%.

3.5 Raman spectra measurement

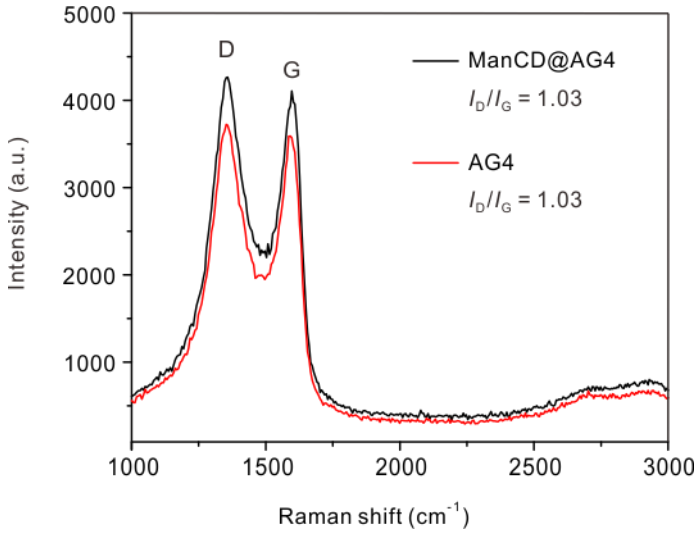

Figure S8. Raman spectra of AG4. The characteristic peaks of graphene around 1600 cm^{-1} (G band) and 1350 cm^{-1} (D band) are related to the in-plane vibration of sp^2 carbon atoms in a 2D hexagonal lattice, and the vibrations of sp^3 carbon atoms of disordered graphite, respectively. The ratio of I_D/I_G indicates the degree of defects on the graphene sheet.

3.6 Morphology investigation of AG4 by AFM

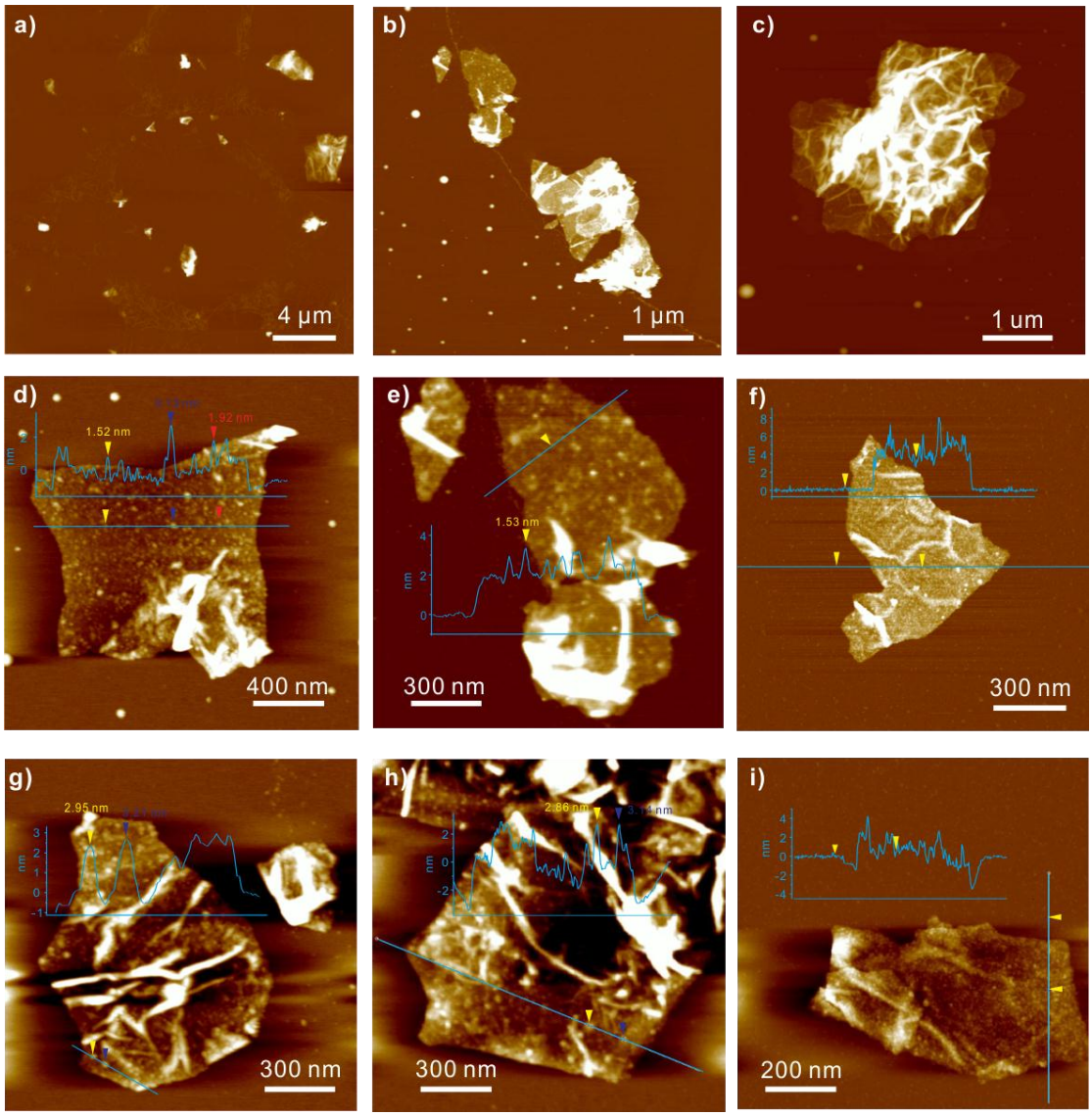

Figure S9. AFM images of sample AG4 at different magnifications. In order to fairly evaluate the morphology and height profiles of AG4 carbon sheets, several areas were randomly picked up for analysis. As depicted in Figure S9, the decoration of adamantyl chain increase the dispersibility of AG4, since we can easily observe many paper-like carbon sheets (d-i), with diverse sizes ranging from hundreds nanometers to several micrometers. Some severe aggregated sheets remain observed (c). It should be noted that in majority of well-dispersed AG4 sheets, many small dots can be detected on the carbon surface (indicated by colored inverted triangle). Due to the limited resolution of AFM images (the error bar of height profile is ±1 nm), the height of these dots is around 2-3 nm, which could be ascribed to the adamantyl chains attached on the surface.

3.7 Morphology investigation of AG4 by TEM

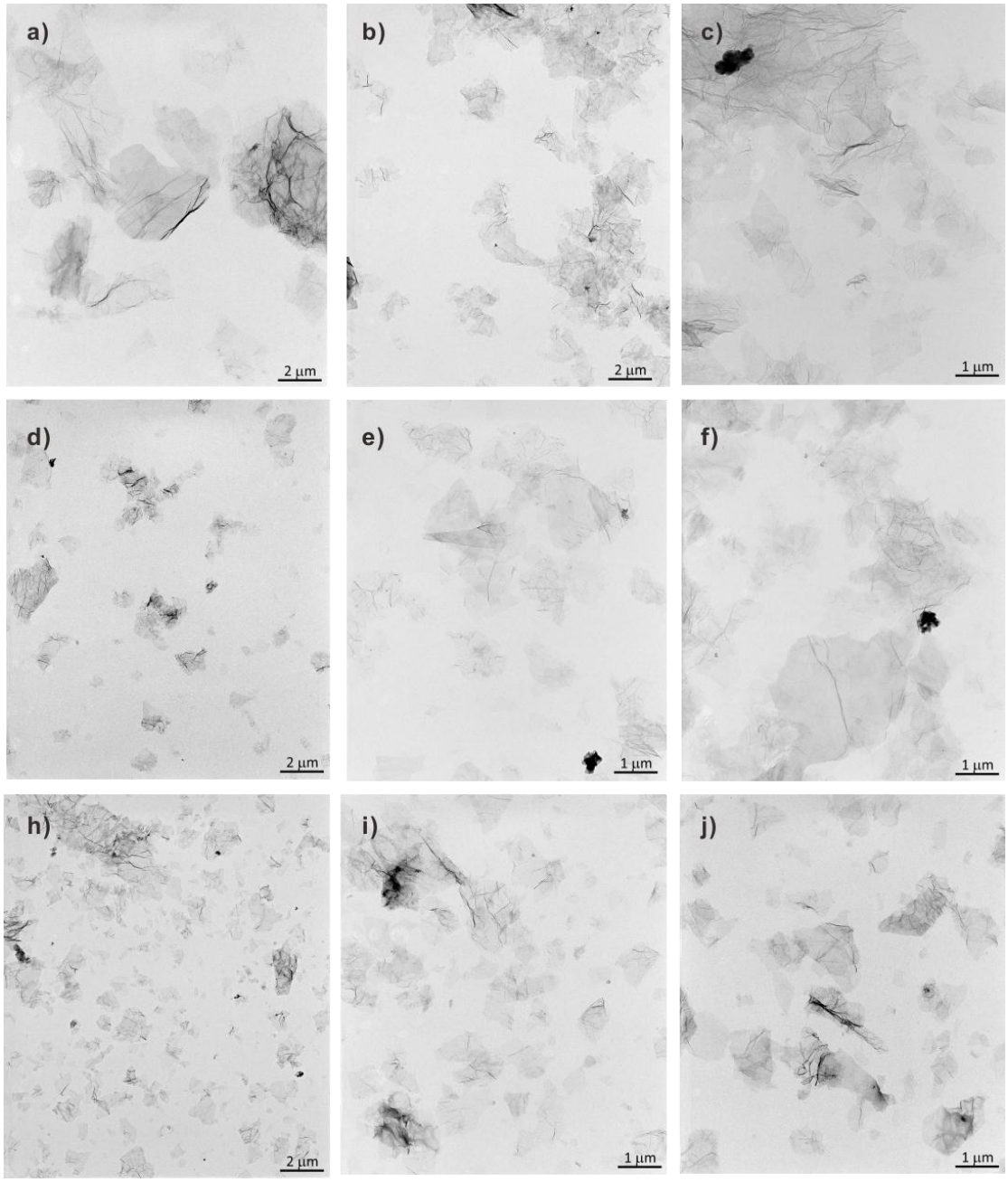

Figure S10. TEM images of sample AG4 collected by different speed of centrifugation: (a-c) the precipitated portion collected at the centrifugation cut-off of (a-c) 2000 rpm, (d-f) 4000 rpm and (h-j) 6000 rpm. In analogy with the AFM observation in Figure S9, we can easily observe many paper-like carbon sheets, with diverse sizes ranging from hundreds nanometers to several micrometers.

3.7 Morphology investigation of AG7 by AFM

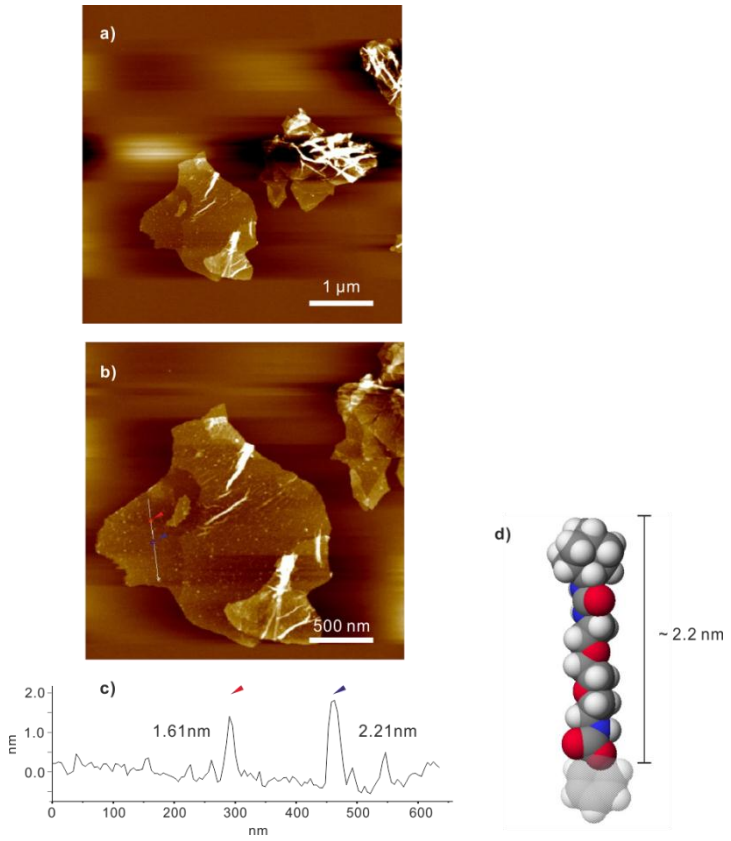

Figure S11. AFM images of AG7 prepared at different magnification. As shown in Figure S11, it is much easier to find the paper-like flat carbon sheets. Due to the fewer number of hydroxyl groups graphene surface, the AG7 carbon sheets have fewer defects (more sp^2 carbon) and less distortion. Accordingly, it is easy to understand the morphology of AG7 is more flat than that of AG4. The reduced roughness of surface leads to the higher resolution of the height profiles. As shown Figure S11c, the derivation of surface background is less than 1 nm (± 0.5 nm). Again, many small dots were also detected on the surface of AG7. The height of these dots is determined to be ~2 nm (e.g. 1.6 nm – 2.2 nm), which is in consistent with the calculated length of fully stretched adamantyl-(ethylenedioxy)bis(ethylamine)-based linker (~2.2 nm, calculated by CaChe program at the AM1 MOZYME level of theory, see Fig. S11d). This result further confirms the small dots observed in Figure S9 are these adamantly-linkers.

4. Characterization of supramolecular carbohydrate-functionalized graphene

4.1 Solubility test of ManCD@AG4 and CD@AG4

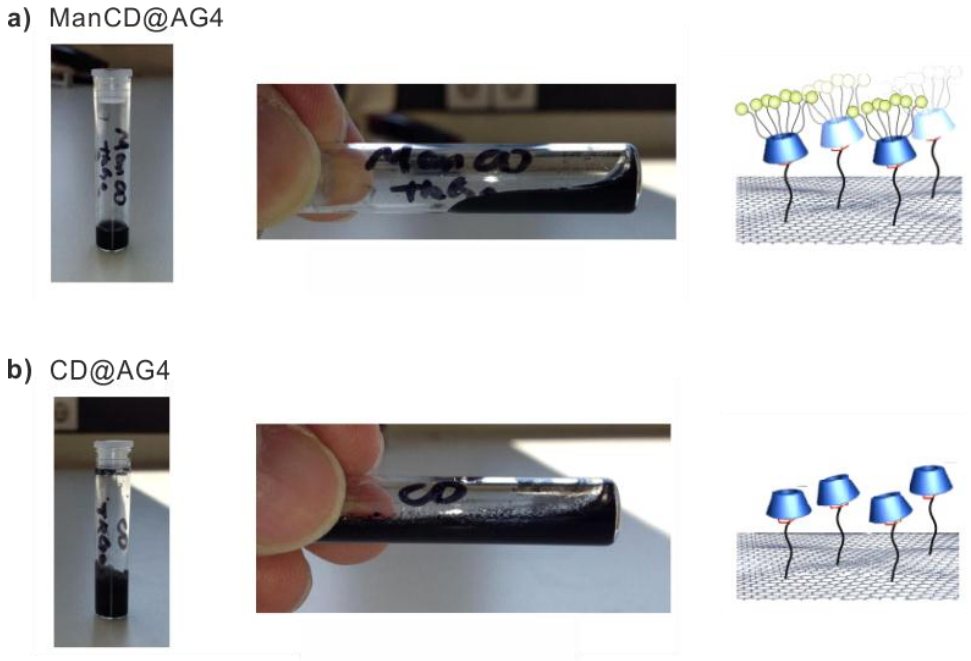

Figure S12. Photographs of a) ManCD@AG4 and b) CD@AG4 dispersed in Milli-Q water. With the functionalization of ManCD, the resulting ManCD@AG4 (98.2 μM, calculated based on ß-CD unit) exhibits higher solubility in water. The ManCD@AG4 is homogenous black liquid. In the contrast, the CD@AG4 with identical concentration has limited solubility. Many agglomerates of fine particle are visible.

4.2 Morphology investigation of ManCD@AG4 by AFM

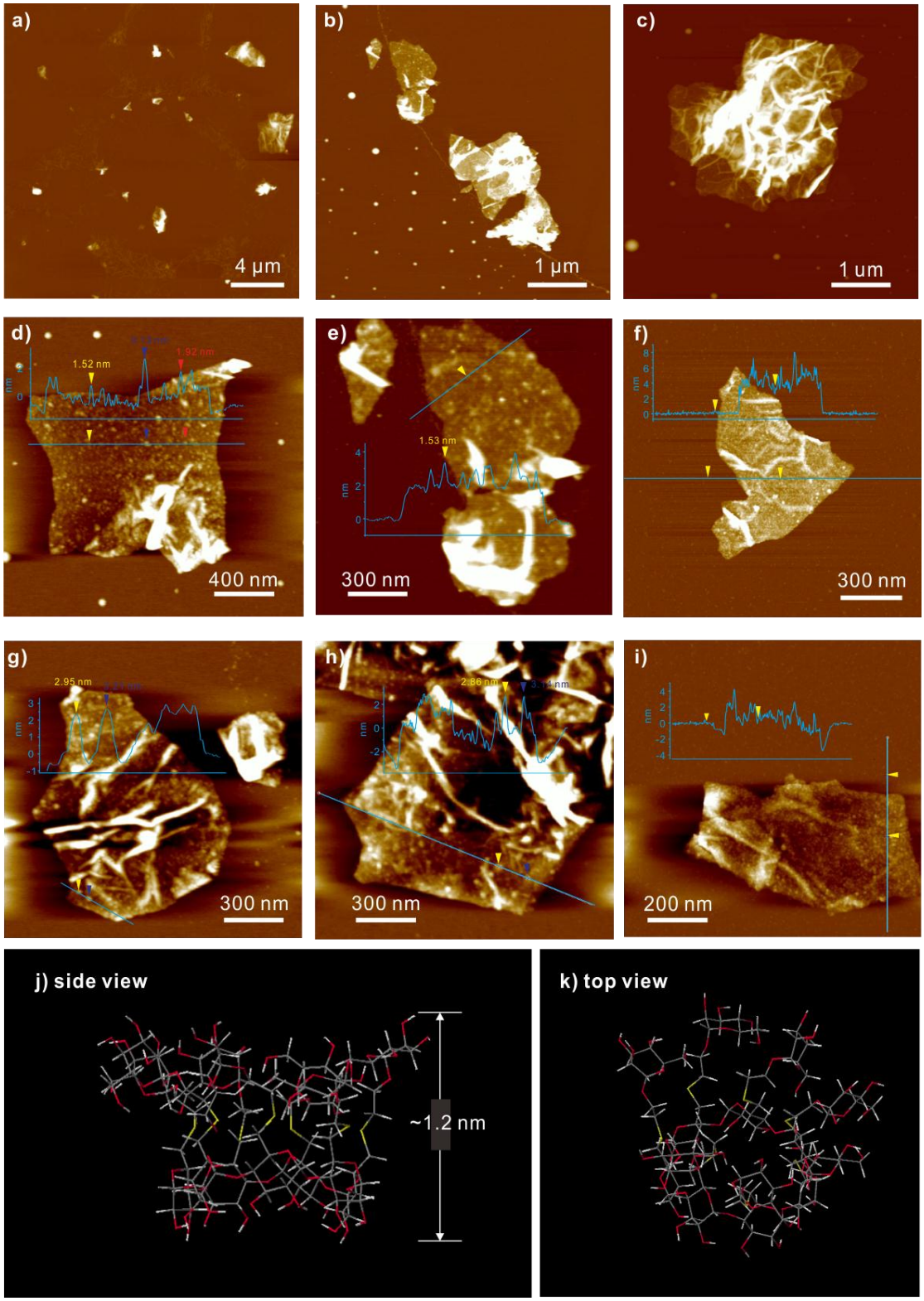

Figure S13. AFM height images (a-i) of sample ManCD@AG4 prepared by spin-coating of solution. Based on AFM data, the height of ManCD@AG4 is in the range of 4 – 5 nm. In comparison with the height of AG4 and ManCD@AG4, the increased height is around 1 nm,

which is in agreement with the calculated height of ManCD (j-k) calculated by CaChe program at the AM1 MOZYME level of theory. The increased height of ManCD@AG4 indicates the host-guest complexation occurs on the adamantyl functionalized graphene surface.

4.3 Morphology investigation of ManCD@AG4 by TEM

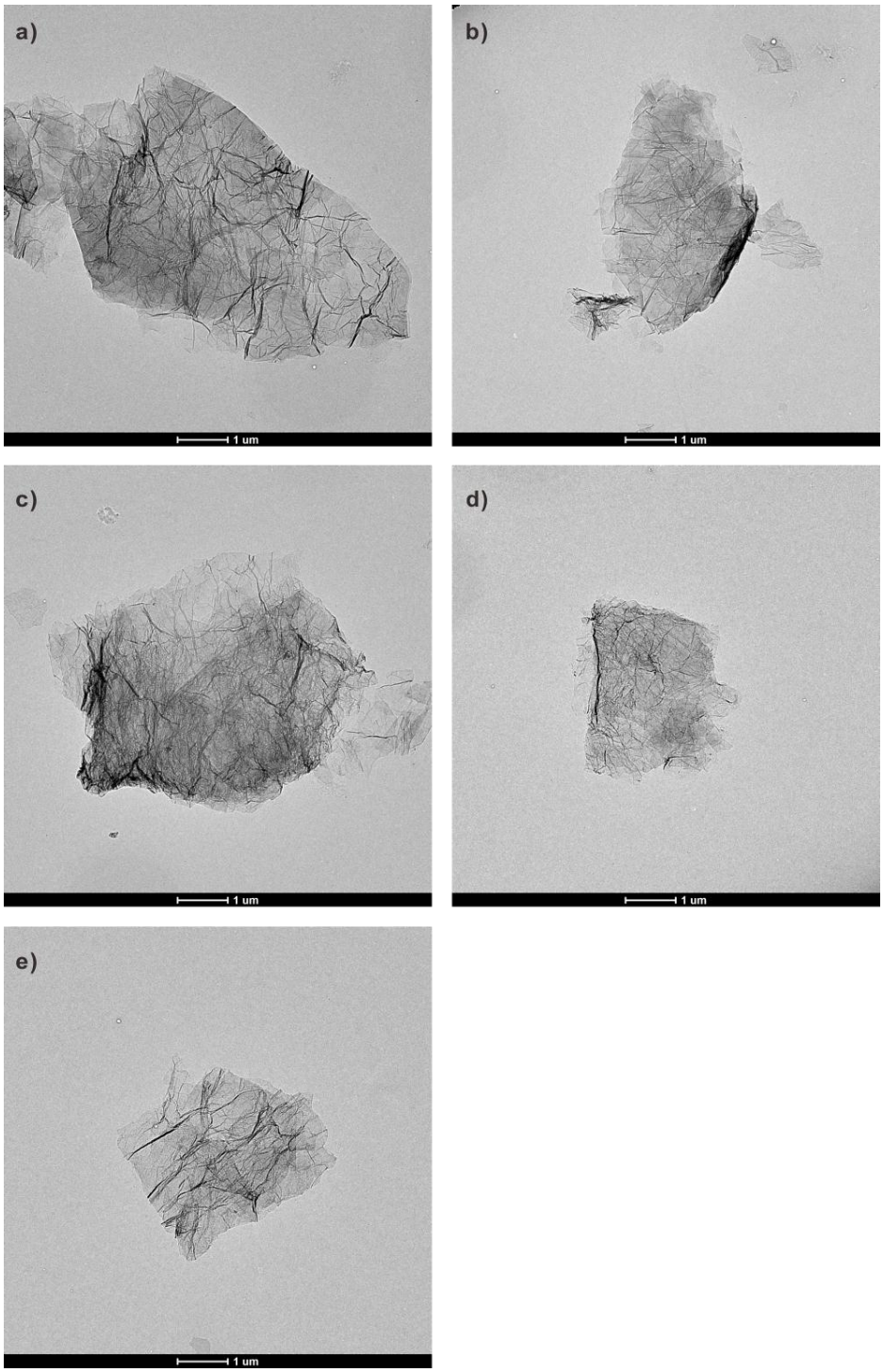

Figure S14. TEM images of sample ManCD@AG4.

4.4 Control experiment demonstrating the host-guest complexation in ManCD@AG4

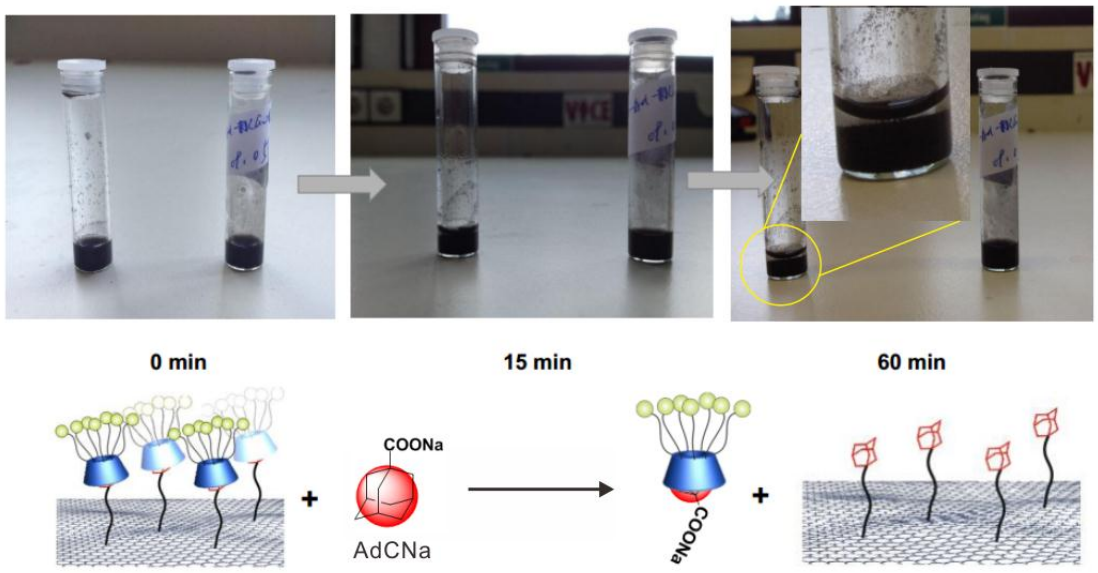

Figure S15 Control experiment demonstrating the complexation. Upon the addition of large excess competitive guest AdCNa (100 eq.), the ManCD is occupied by the AdCNa, thus expelled from the AG4 surface. As expected, the dissociation of of ManCD@AG4 results in the precipitation of AG4 in water. This result further confirms the host-guest complexation occurs on the graphene surface.

4.5 Determination of the amount of attached carbohydrate on graphene surface

Anthrone is used for a popular cellulose assay and in the colorometric determination of carbohydrates.[6] ManCD@AG4, CD@AG4 and AG4 were dispersed in deionized water (0.5 mL) in an ice bath. A freshly prepared 0.5% (w/w) solution of anthrone in sulfuric acid (1 mL) was added slowly to this solution. The resulting solution was gently mixed and heated to 80 °C for 10 min. The absorption of the solution was measured at 620 nm and compared with those that were obtained from a standard curve to determine the amount of ligand on the ManCD@AG4 surface.

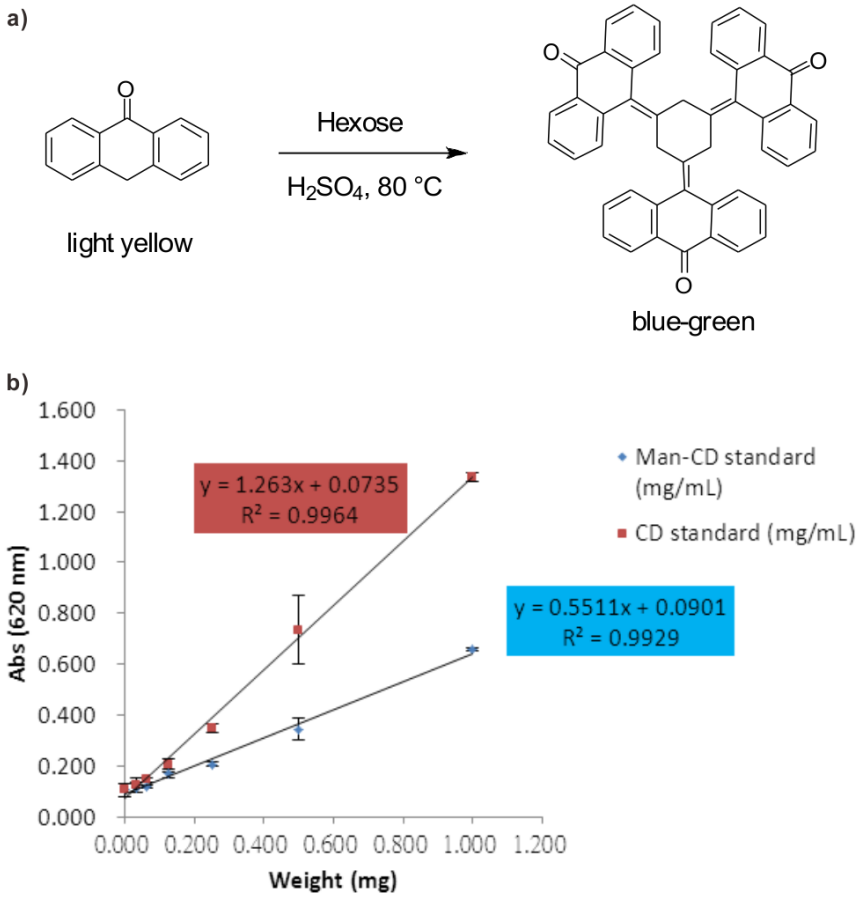

Figure S16 A standard deviation curve estimate the sugar amount (i.e. CD unit) on ManCD@AG4 is 117.8 ± 8.7 nmol/mg, and CD@AG4 is 109.2 ± 7.7 nmol/mg, according to AG4 weight.

5. *E.coli* capture effect by sugar-functionalized graphene derivatives

5.1 TEM observation of E.coli strains with ManCD@AG4

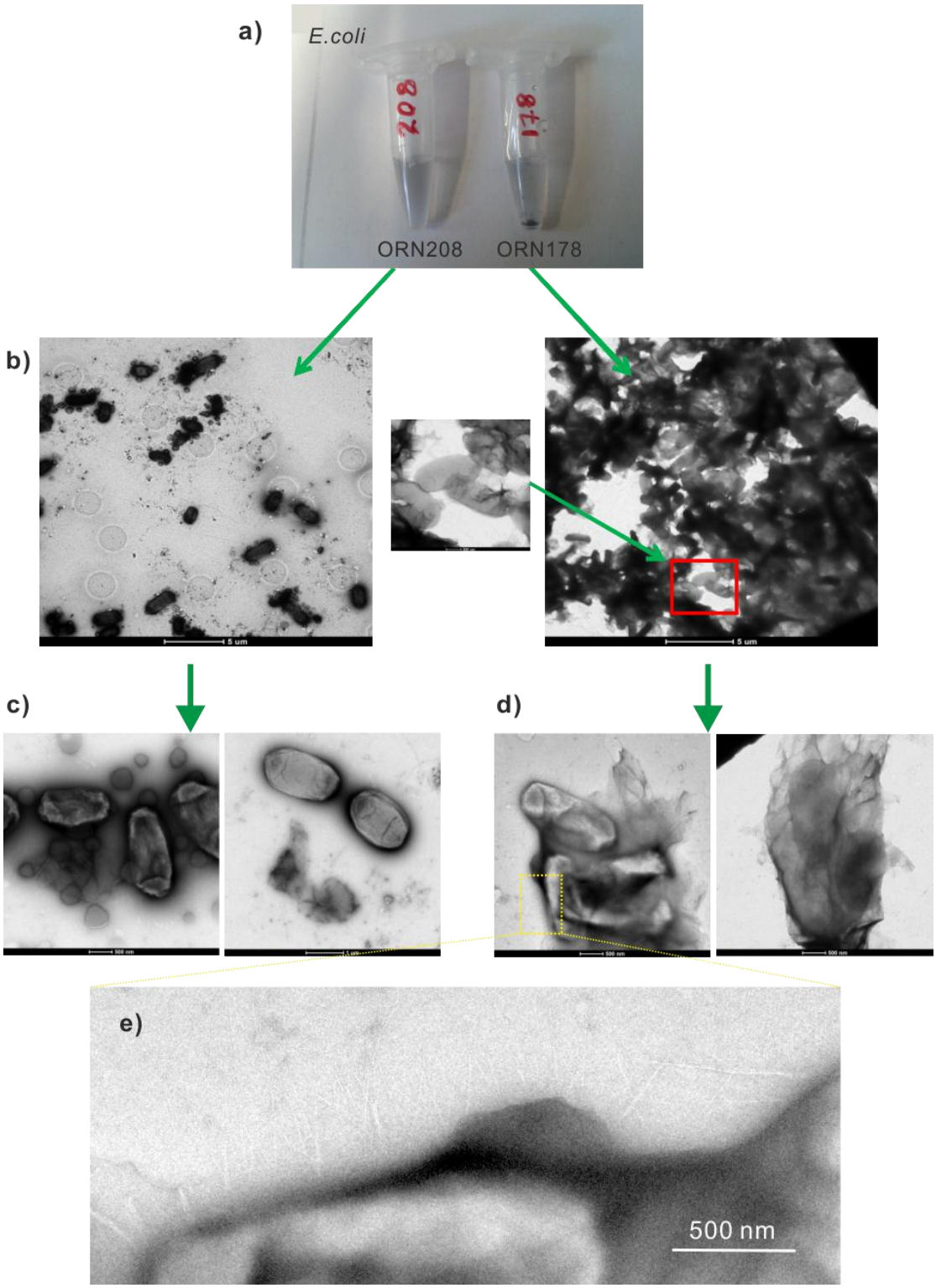

Figure S17 a) Enlarged imgaes for the comparison of different response of ManCD@AG4 after the addition of *E.coli* strain ORN208 and strain ORN178 respectively, after incubation for 1 hour at room temperature. b) Overview of the TEM image at ManCD@AG4 and *E.coli* strain ORN208

and strain ORN178 at the same magnification (5 μm scale bar). The Magnified TEM images of ManCD@AG4 interacting with of *E.coli* strain c) ORN208 and d) ORN178 (The scale bar of image at 500 nm and 1 μm), respectively. e) Enlarged domain for TEM image in d).

5.2 Visualization of E.coli strain ORN178 with ManCD@AG4 by stereoscopic TEM

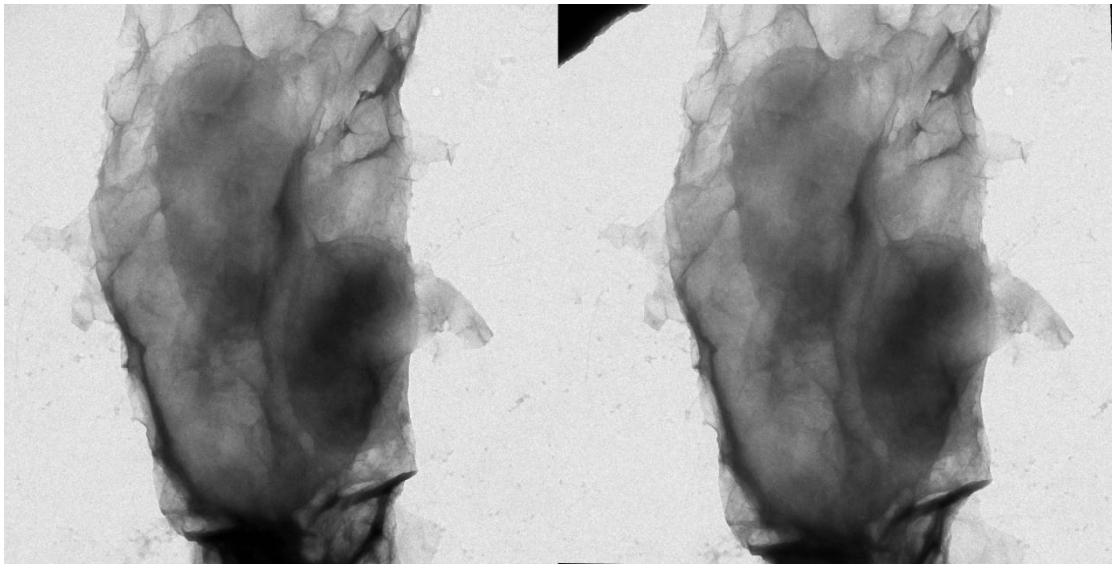

Figure S18 *E.coli* strain ORN178 incubated with ManCDAG4 which is in complementary to Figure 1c in the maintext. TEM stereo images (side-by-side stereogram) at an 8° view angle.

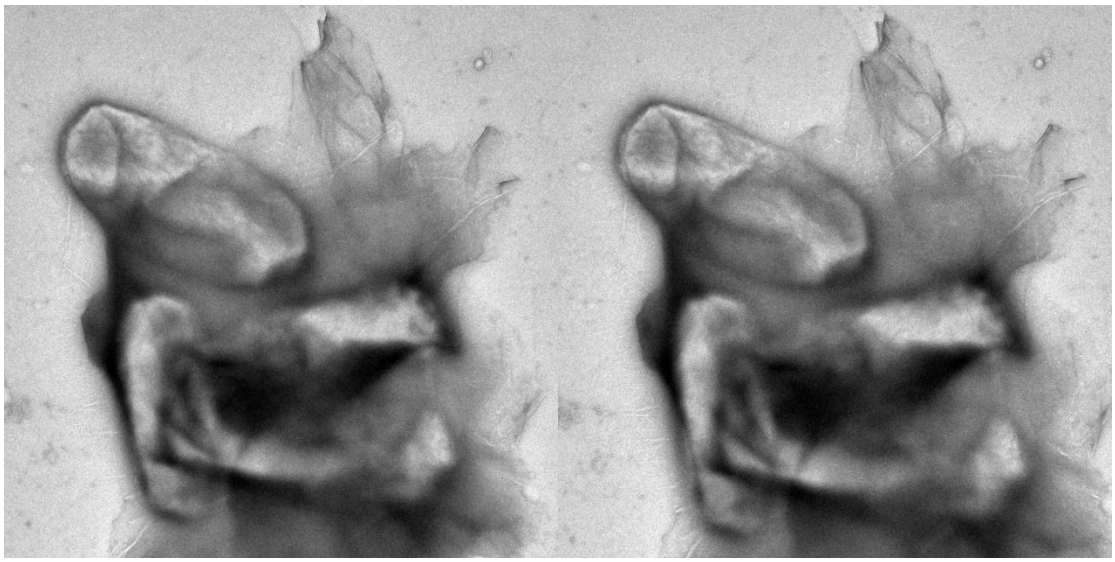

Figure S19 *E.coli* strain ORN178 incubated with ManCDAG4, which is in complementary to Figure S17d. TEM stereo images (side-by-side stereogram) at an 8° view angle.

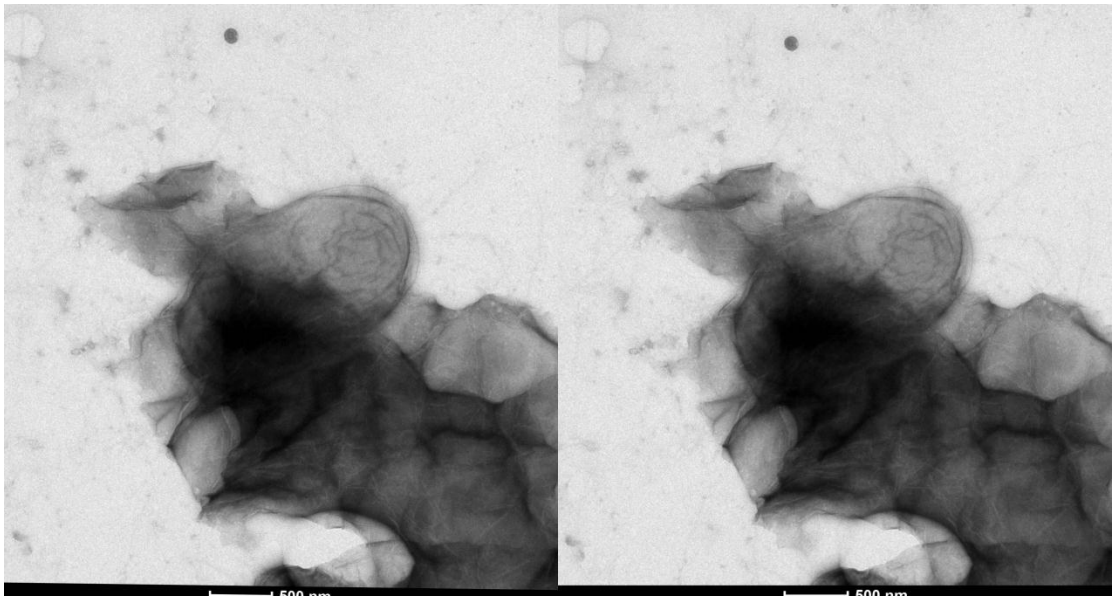

Figure S20 Additional *E.coli* strain ORN178 incubated with ManCDAG4. TEM stereo images (side-by-side stereogram) at an 8° view angle. The bacteria is wrapped inside ManCD@AG4.

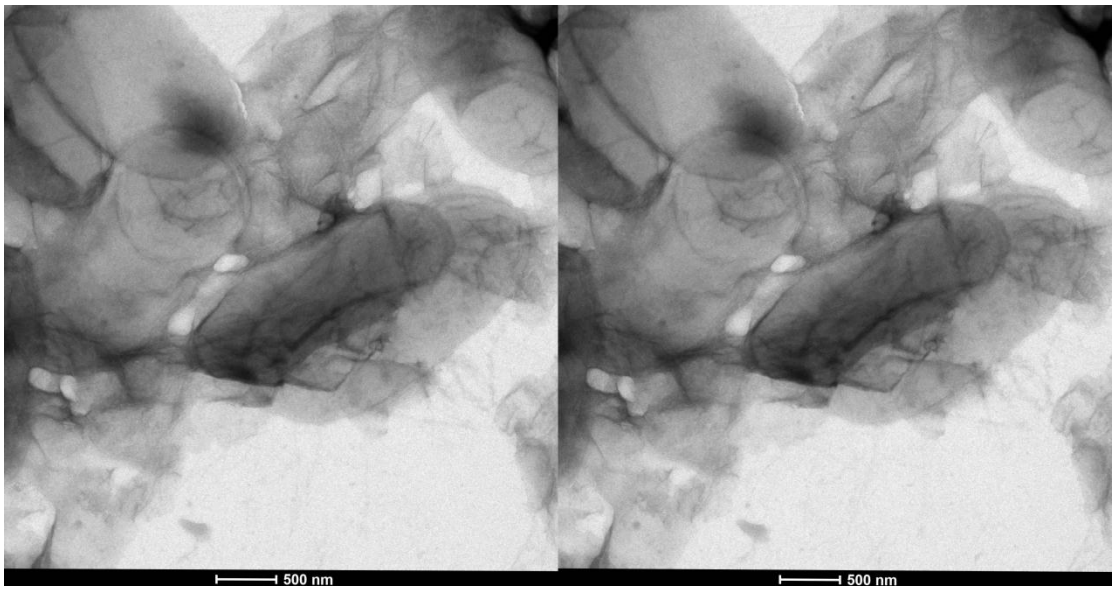

Figure S21 Additional *E.coli* strain ORN178 incubated with ManCDAG4. TEM stereo images (side-by-side stereogram) at an 8° view angle. The bacteria is wrapped inside ManCD@AG4.

5.3 Confocal laser scanning microscopy observation of E.coli strains with ManCD@AG4 and CD@AG4 respectively

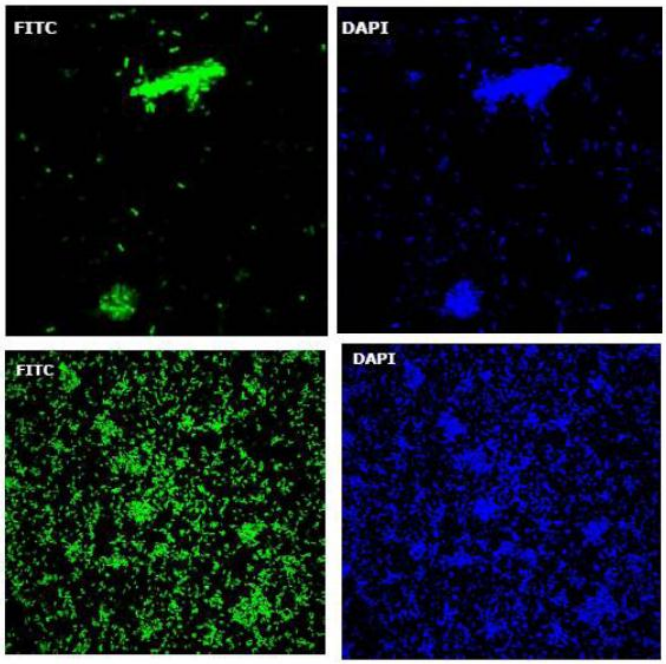

Figure S22 Confocal laser scanning microscopy images for the incubation of ManCD@AG4 with bacteria *E.coli* strain ORN178 (top row) and of ORN208 (bottom row).

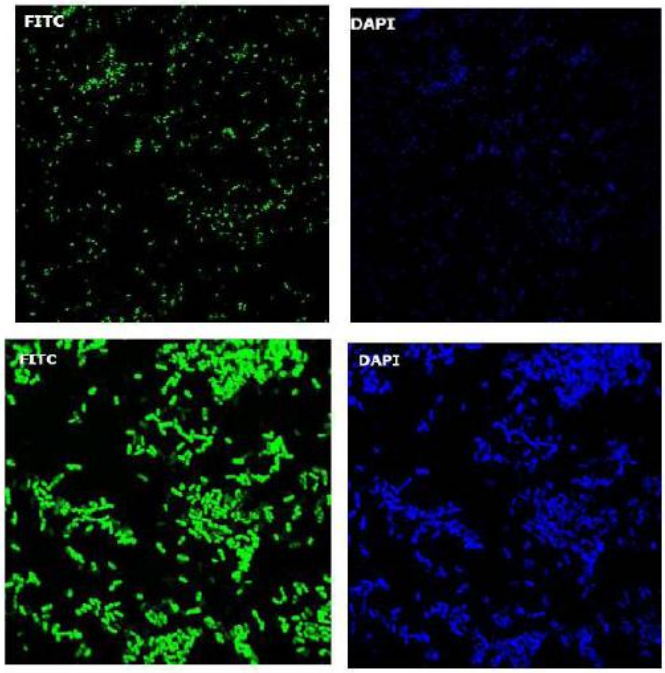

Figure S23 Confocal laser scanning microscopy images for the incubation of CD@AG4 with bacteria *E.coli* strain ORN178 (top row) and of ORN208 (bottom row). In line with the repeated experiment shown in Figure 2a-d in maintext, the selective capture effect is highly reproducible.

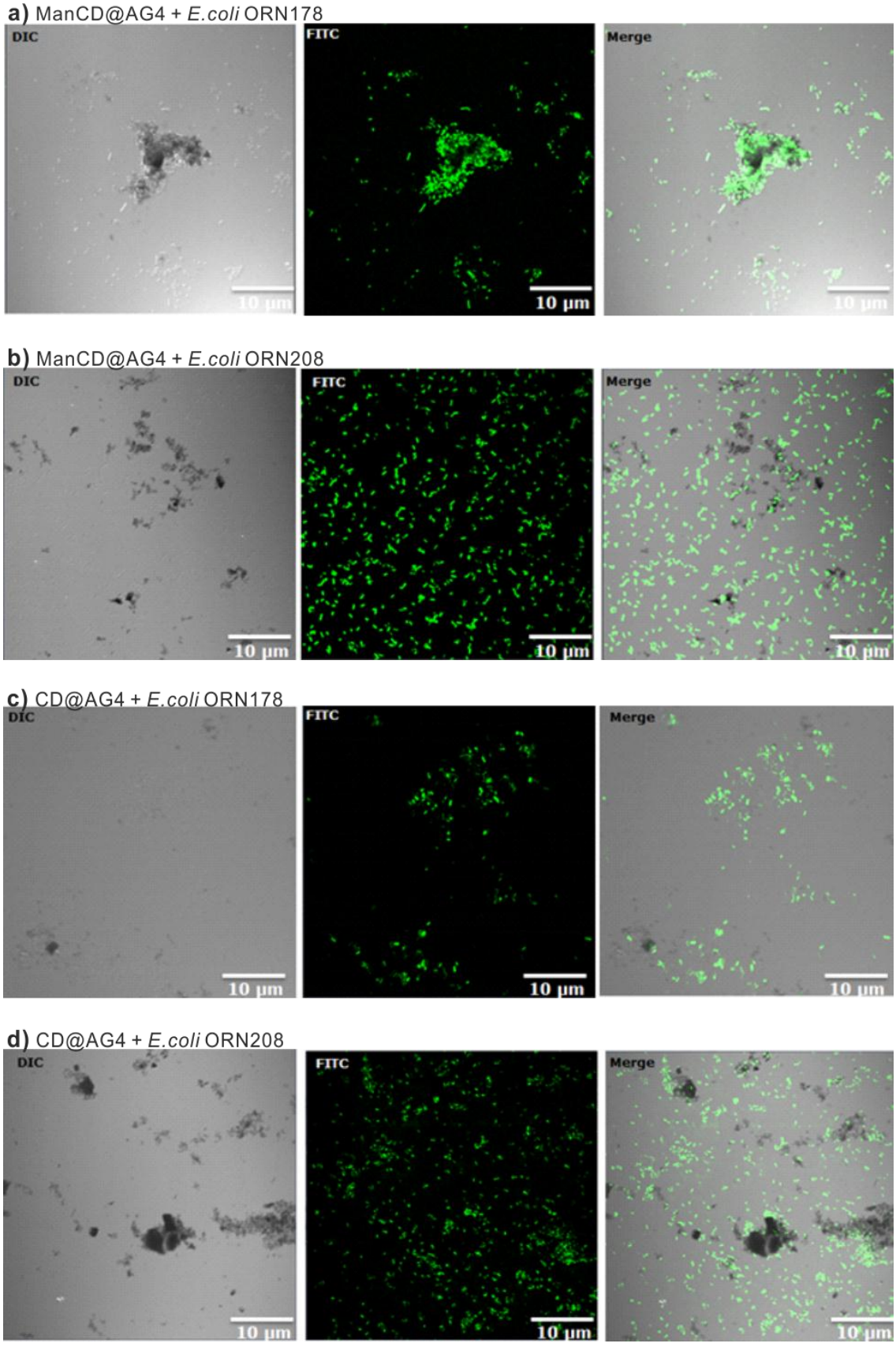

Figure S24 Repeated confocal laser scanning microscopy images for the incubation of bacteria a) *E.coli* strain ORN178 with ManCD@AG4; b) ORN208 with ManCD@AG4; c) ORN178 with

CD@AG4, and d) ORN208 with CD@AG4 as negative controls.

5.4 Methods for calculating agglutination index (A.I.)

According to previous reported protocol,[7] the agglutination indexes (A.I.) were calculated from 10 random fields of confocal microscopic images. The number of cells in close contact was indicated by the fluorescent intensity of aggregation (FL_{agg}) which was readout by the cell counting software Image-Pro Plus (version 6.0, trail). The fluorescent intensity of non-aggregated cell was also recorded and averaged as FL_{single}. After summing of FL_{agg} from 10 random fields of confocal microscopic images ($\sum_i^{10} FL_{agg}(i)$), and then divide the FL_{single} , as:

$$\text{A.I.} = \frac{\sum_i^{10} FL_{agg}(i)}{FL_{single}} \qquad \text{(eq.S1)}$$

In accordance with the case of ManCD@AG4 and *E.coli* strain ORN178, other sample cases mentioned in the maintext was calculated by the same method.

6. *E.coli* killing effect by NIR laser irradiation with sugar-functionalized graphene derivatives

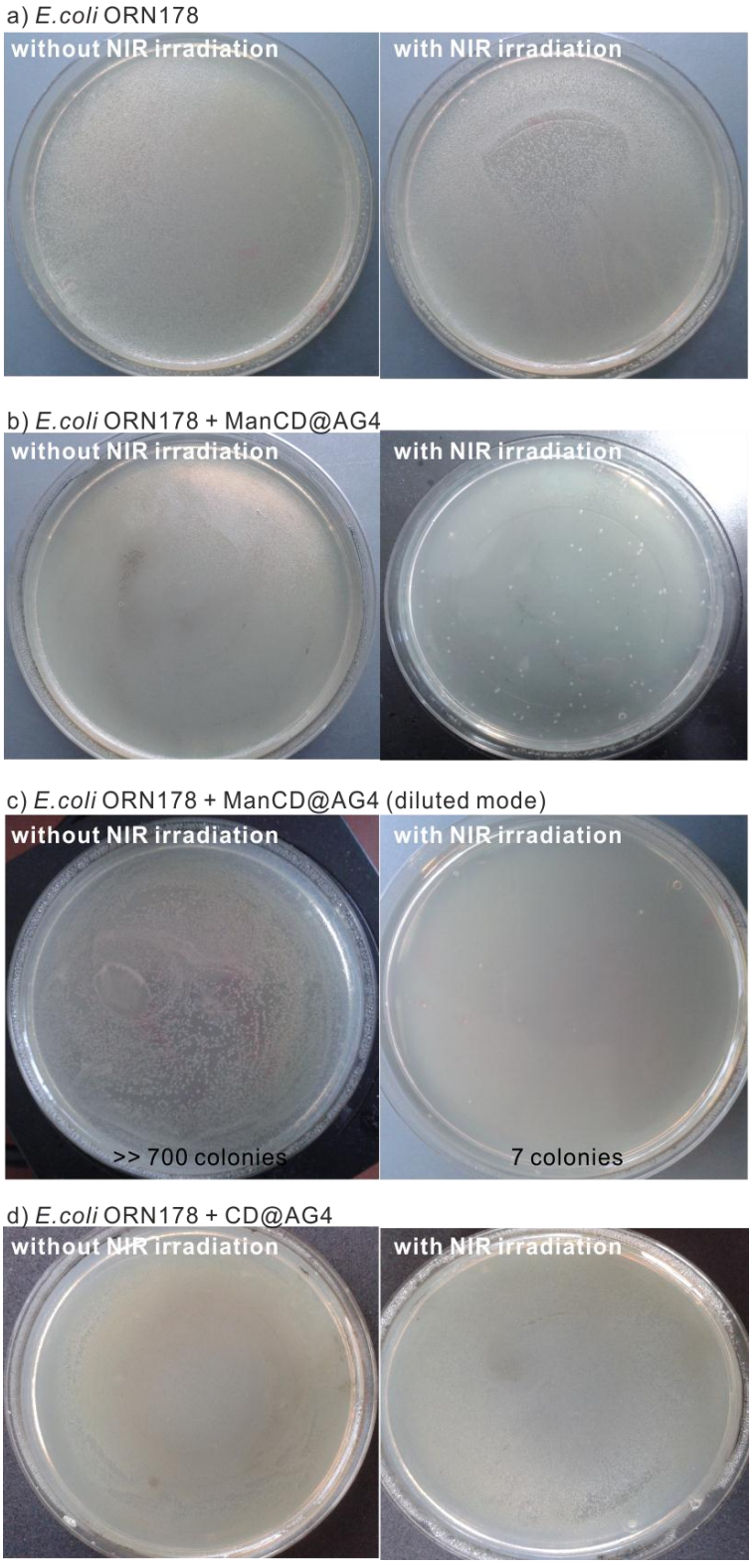

Figure S25 The compared photographs of *E.coli* bacterial colonies interacting with a) none; b-c) ManCD@AG4; d) CD@AG4 without (left) and with (right) NIR laser irradiation. In comparison with *E.coli* only (Figure S6a), and *E.coli* incubated with CD@AG4 (Figure S6d), the growth of

E.coli with ManCD@AG4 on the agar plates (Figure S6b-c) is significantly reduced due to the 10 min NIR laser irradiation (785 nm), in which very few colonies were observed. In the diluted mode, The killing efficiency number was derived from the colony counting number (see Figure S6c), that the killing efficiency towards *E.coli* is > 99%.

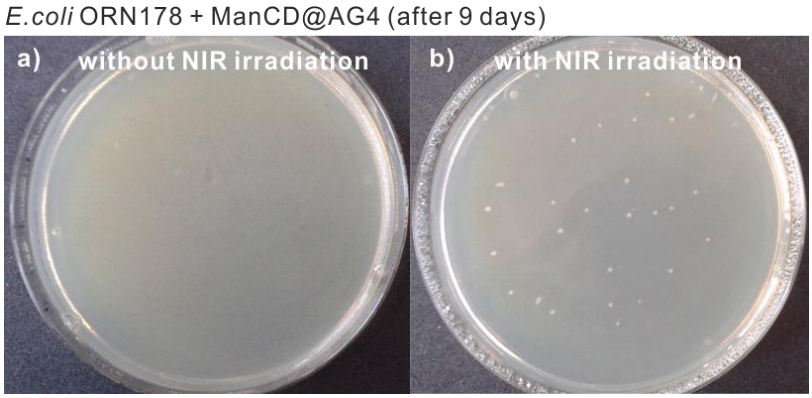

Figure S26 Evaluation of the long term inhibition of growth of bacteria on the NIR irradiation *E.coli* sample (interacting with ManCD@AG4). The photographs of *E. coli* bacterial colonies were taken from the re-cultured samples which has been kept at 4℃ for 9 days: a) *E.coli* ORN178 incubated with ManCD@AG4 without NIR treatment; b) *E.coli* ORN178 incubated with ManCD@AG4 with NIR treatment. As shown in Figure S7b, the NIR radiation is able to disinfect the *E.coli* and only very little colonies (38 colonies) was observed. In contrast, the sample without NIR radiation, the *E.coli* grew full of the agar plate.

7. Reference

1. Z. Qi, P. Malo de Molina, W. Jiang, Q. Wang, K. Nowosinski, A. Schulz, M. Gradzielski and C. A. Schalley, *Chem. Sci.*, 2012, **3**, 2073-2082.

2. W. S. Hummers, R. E. Offeman, *J. Am. Chem. Soc.* **1958**, *80*, 1339-1339.

3. a) A. García-Barrientos, J. J. García-López, J. Isac-García, F. Ortega-Caballero, C. Uriel, A. Vargas-Berenguel, F. Santoyo-González, *Synthesis* **2001**, *2001*, 1057-1064: b) D. Grünstein, M. Maglinao, R. Kikkeri, M. Collot, K. Barylyuk, B. Lepenies, F. Kamena, R. Zenobi, P. H. Seeberger, *J. Am. Chem. Soc.* **2011**, *133*, 13957-13966.

4. A.-K. Appel, R. Thomann, R. Mülhaupt, *Polymer* **2012**, *53*, 4931-4939.

5. A.-K. Appel, PhD thesis, University of Freiburg **2013**, p38.

6. C.-H. Lai, N.-C. Lai, Y.-J. Chuang, F.-I. Chou, C.-M. Yang, C.-C. Lin, *Nanoscale* **2013**, *5*,

9412-9418.

7. a) Y.-b. Lim, S. Park, E. Lee, J.-H. Ryu, Y.-R. Yoon, T.-H. Kim, M. Lee, *Chem. Asian J.* **2007**, *2*, 1363-1369; b) G. Yu, Y. Ma, C. Han, Y. Yao, G. Tang, Z. Mao, C. Gao, F. Huang, *J. Am. Chem. Soc.* **2013**, *135*, 10310-10313.